# Intermolecular Ferromagnetic and Antiferromagnetic Interactions in Halogen-Bridged Copper(I) Imino Nitroxides: Crystal Structures and Magnetic Properties of $[Cu^{I}(\mu\text{-X})(\text{imino nitroxide})]_2$ (X = I or Br)

**Hiroki Oshio,*,† Takashi Watanabe,† Akihiro Ohto,† Tasuku Ito,*,† and Hideki Masuda‡**

Department of Chemistry, Faculty of Science, Tohoku University, Aoba-ku, Sendai 980-77, Japan, and Department of Applied Chemistry, Nagoya Institute of Technology, Showa-ku, Nagoya 466, Japan

*Received May 26, 1995*[⊗]

Reaction of CuI or CuBr with some imino nitroxides in methanol gave the halogen bridged dinuclear Cu(I) complexes $[Cu(\mu\text{-I})(impy)]_2$ (**1**), $[Cu(\mu\text{-I})(immepy)]_2$ (**2**), $[Cu(\mu\text{-Br})(immepy)]_2$ (**3**), and $[Cu(\mu\text{-Br})(imph\text{-}NO_2)]_2$ (**4**), respectively (impy = 2-(2′-pyridyl)-4,4,5,5-tetramethyl-4,5-dihydro-1*H*-imidazolyl-1-oxyl, immepy = 2-(6′-methyl-2′-pyridyl)-4,4,5,5-tetramethyl-4,5-dihydro-1*H*-imidazolyl-1-oxyl, imph-$NO_2$ = 2-(4′-nitrophenyl)-4,4,5,5-tetramethyl-4,6-dihydro-1*H*-imidazolyl-1-oxyl). Crystal structures and magnetic properties have been studied. Complexes **1**−**4** have dimeric structures where two copper ions are doubly bridged by halide ions in a $\mu_2$ fashion. In **1**−**3**, each copper ion is tetrahedral with a bidentate imino nitroxide and two halide ions, and the two copper ions are separated by 2.592(2), 2.6869(8), and 2.7357(6) Å, respectively. In **4**, triangular coordination sites of the copper ions are completed with a nitrogen atom from the imino nitroxide and two bromide ions bridging the two copper ions with a separation of 3.074(2) Å. Ligand imino nitroxides in **1**−**4** form one-dimensional radical chains, and the chains are linked with halocuprate dimer units. Structural and magnetic susceptibility data support that radicals in **1** and **4** are ferromagnetically stacked, while radicals in **2** and **3** form an antiferromagnetic chain. The magnetic behaviors are discussed in connection with the stacking modes of the radicals and bridging conformations. Crystal data (Mo Kα, $\lambda = 0.71069$ Å): **1**, orthorhombic, space group $P2_12_12_1$, $a = 17.807(2)$ Å, $b = 8.595(2)$ Å, $c = 19.336(6)$ Å, and $Z = 4$; **2**, monoclinic, space group $P2_1/c$, $a = 9.941(2)$ Å, $b = 18.482(2)$ Å, $c = 8.337(2)$ Å, $\beta = 96.41(2)°$, and $Z = 2$; **3**, monoclinic, space group $P2_1/c$, $a = 9.964(6)$ Å, $b = 18.167(4)$ Å, $c = 8.009(7)$ Å, $\beta = 95.81(6)°$, and $Z = 2$; **4**, monoclinic, space group $P2_1/c$, $a = 11.991(7)$ Å, $b = 17.998(8)$ Å, $c = 7.215(6)$ Å, $\beta = 104.07(6)°$, and $Z = 2$.

## Introduction

There has been increasing interest in molecular assemblies which have macroscopic properties like ferromagnetism. Since the first molecular-based ferromagnets $[Fe(C_5H_5)_2][TCNE]$[1] and $[MnCu(pba)(H_2O)_3]\cdot 2H_2O$[2] in 1986 have been reported, several ferro- and ferrimagnets were reported. In particular, combinations of metal complexes and nitroxides have been proven to be good components for building such magnetic materials. Actually, $[M(hfac)_2][NITR]$ (M = $Mn^{II}$, $Ni^{II}$ and hfac = hexafluoroacetylacetone),[3] $[polynitroxide]_2[Mn(hfac)_2]_3$,[4] and $(radical)_2Mn_2[Cu(opba)]_3(DMSO)_2\cdot 2H_2O$[5] have been reported to show spontaneous magnetization at 10, 3.4, and 22.5 K, respectively. A key point to having such macroscopic properties in solids is to have strong intermolecular interactions.

Diamagnetic metal ions have been believed not to mediate magnetic interactions. Some diamagnetic metal complexes with organic radicals as a ligand, however, have shown that ferromagnetic interactions were operative through the diamagnetic metal ions. In $Ti^{IV}$−[6] and $Ga^{III}$−semiquinone complexes,[7] for example, the semiquinone ligands show ferromagnetic interaction ($J = -56$ cm$^{-1}$; $H = JS_1S_2$ and 7.8 cm$^{-1}$; $H = -2\sum JS_iS_j$, respectively). We have also shown that a copper(I) ion in $[Cu^{I}(immepy)_2](PF_6)$ (immepy = bidentate imino nitroxide) mediates rather strong intramolecular ferromagnetic coupling ($2J = 102$ cm$^{-1}$; $H = -2JS_1S_2$) between the coordinating radicals.[8] If the certain conditions are fulfilled, these diamagnetic metal ions are considered to be particularly suitable for linking organic radicals. On the other hand, copper(I) halocuprates display a wide variety in structures. These molecules form discrete geometries of varying nuclearity or polymeric extended systems.[9] If organic radicals are introduced into the halocuprate cluster or network, interesting magnetic materials might be obtained. We report here the syntheses, crystal structures, and

† Tohoku University.
‡ Nagoya Institute of Technology.
[⊗] Abstract published in *Advance ACS Abstracts,* December 15, 1995.

(1) Miller, J. S.; Calabrese, J. C.; Bigelow, R. W.; Epstein, A.; J. Zhang, R. W.; Reiff, W. M. J. *Chem. Soc., Chem. Commun*. **1986**, 1026.
(2) Pei, Y.; Verdaguer, M.; Kahn, O.; Sletten, J.; Renard, J. P. *J. Am. Chem. Soc*. **1986**, *108*, 7428.
(3) (a) Caneschi, A.; Gatteschi, D.; Renard, J. P.; Rey, P.; Sessoli, R. *J. Am. Chem. Soc.* **1989**, *111*, 785. (b) Caneschi, A.; Gatteschi, D.; Renard, J. P.; Rey, P.; Sessoli, R. *Inorg. Chem*. **1989**, *28*, 1976. (c) Caneschi, A.; Gatteschi, D.; Renard, J. P.; Rey, P.; Sessoli, R. *Inorg. Chem*. **1989**, *28*, 3314. (d) Caneschi, A.; Gatteschi, D.; Renard, J. P.; Rey, P.; Sessoli, R. *Inorg. Chem*. **1989**, *28*, 2940.
(4) Inoue, K; Iwamura, H. *J. Am. Chem. Soc*. **1994**, *116*, 3173.
(5) (a) Stumpf, H. O.; Ouahab, L. Pei, Y.; Grandjean, D.; Kahn, O. *Science* **1993**, *261*, 447. (b)Stumpf, H. O.; Ouahab, L. Pei, Y.; Bergerat, P.; Kahn, O. *J. Am. Chem. Soc*. **1994**, *116*, 3866.
(6) (a) Caneschi, A.; Dei, A.; Gatteschi, A. *J. Chem. Soc., Chem. Commun*. **1992**, 630. (b) Bruni, S.; Caneschi, A.; Cariati, F.; Delfs, C.; Dei, A.; Gatteschi, D. *J. Am. Chem. Soc*. **1994**, *116*, 1388.
(7) Adams, D. M.; Rheingold, A. L.; Dei, A.; Hendrickson, D. N. *Angew. Chem., Int. Ed. Engl*. **1993**, *32*, 391.
(8) Oshio, H.; Watanabe, T.; Ohto, A.; Ito, T.; Nagashima, U. *Angew. Chem., Int. Ed. Engl*. **1994**, *33*, 670.
(9) (a) Subramanian, L.; Hoffmann, R. *Inorg. Chem*. **1993**, *31*, 1021. (b) Vitale, M.; Ryu, C. K.; Palke, W. E.; Ford, P. C. *Inorg. Chem*. **1994**, *33*, 561. (c) Raston, C. L.; White, A. H.; White, A. H. *J. Chem. Soc., Dalton Trans*. **1976**, 2153. (d) Andersson, S.; Jagner, S. *Acta Chem. Scand. A* **1986**, *40*, 177. (e) Jagner, S.; Helgesson, G. *Adv. Inorg. Chem*. **1991**, *37*, 1. (f) Bowmaker, G. A. *Adv. Spectrosc*. **1987**, *14*, 1. (g) Bigalke, K. P.; Hans, A.; Hartl, H. *Z. Anorg. Allg. Chem*. **1988**, *563*, 96. (h) Hoyer, M.; Hartl, H. *Z. Anorg. Allg. Chem*. **1990**, *587*, 23.

0020-1669/96/1335-0472$12.00/0 

**Chart 1**

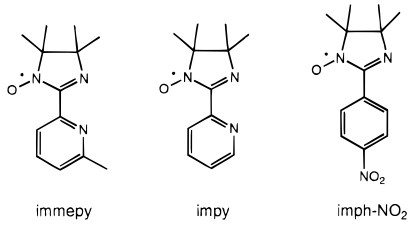


magnetic properties of halogen-bridged dinuclear copper(I) complexes with imino nitroxides, $[Cu^{I}(\mu\text{-}X)(L)]_2$ (X = I or Br and L = impy, immepy, or imph-$NO_2$; see Chart 1).

## Experimental Section

**Preparation of Complexes.** Chemicals used were of reagent grade quality and were used without further purification. All procedures were carried out under a $N_2$ atmosphere by using Schlenk techniques. Ligand imino nitroxides were prepared by the literature method.[10]

**(a) $[Cu(\mu\text{-}I)(impy)]_2$ (1) and $[Cu(\mu\text{-}I)(immepy)]_2$ (2).** To a suspension of 0.19 g (1 mmol) of CuI in 10 mL of methanol was slowly added 0.22 g of impy (1 mmol) or immepy (0.23 g, 0.1 mmol) with stirring, and the solution turned dark red. Upon standing at ambient temperature for 2 days, the mixture deposited dark red tablets. These were filtered off and air-dried, and one of these was subjected to X-ray analysis. Anal. Calcd for **1** for $C_{24}H_{32}Cu_2I_2N_6O_2$: C, 35.26; H, 3.95; N, 10.28. Found: C, 35.20; H, 3.94; N 10.11. Anal. Calcd for **2** for $C_{26}H_{36}Cu_2I_2N_6O_2$: C, 36.93; H, 4.92; N, 9.94. Found: C, 36.22; H, 4.03; N 9.53.

**(b) $[Cu(\mu\text{-}Br)(immepy)]_2$ (3) and $[Cu(\mu\text{-}Br)(imph\text{-}NO_2)]_2$ (4).** To a methanol solution (10 mL) of 0.18 g (0.5 mmol) of $[Cu(CH_3CN)_4](PF_6)$[11] was added 0.103 g (1 mmol) of NaBr. To this suspension of 0.07 g (0.5 mmol) of CuBr was slowly added a methanol solution (10 mL) of immepy (0.12 g, 0.5 mmol) or imph-$NO_2$ (0.13 g, 0.5 mmol). The suspension was stirred at room temperature for 1 h, yielding a dark red solution. After the mixture was allowed to stand overnight, dark red tablets separated from the solution. Anal. Calcd for **3** for $C_{26}H_{36}Cu_2Br_2N_6O_2$: C, 41.55; H, 4.83; N, 11.18. Found: C, 41.35; H, 4.71; N 11.41. Anal. Calcd for **4** for $C_{26}H_{32}Cu_2Br_2N_6O_6$: C, 38.48; H, 3.97; N, 10.36. Found: C, 38.79; H, 3.71; N, 10.51.

**Magnetic Measurements.** Magnetic susceptibility data were collected in the temperature range 2.0−300 K and in applied 10 kG with the use of a Quantum Design Model MPMS SQUID magnetometer. Powdered samples were contained in the small half of a gelatin capsule, and a phenolic guide (clear soda straw) was used to house the sample holder and was fixed to the end of the magnetometer drive rod. $[Cr(NH_3)_6](NO_3)_3$ was employed as duel magnetometer calibrants. Pascal's constants were used to determinate the constituent atom diamagnetism.[12]

**X-ray Crystallography.** Crystals of $[Cu(\mu\text{-}I)(impy)]_2$ (**1**) (dimensions 0.30 × 0.30 × 0.25 mm), $[Cu(\mu\text{-}I)(immepy)]_2$ (**2**) (dimensions 0.30 × 0.20 × 0.15 mm), $[Cu(\mu\text{-}Br)(immepy)]_2$ (**3**) (dimensions 0.30 × 0.30 × 0.40 mm), and $[Cu(\mu\text{-}Br)(imph\text{-}NO_2)]_2$ (**4**) (dimensions 0.30 × 0.30 × 0.25 mm) were used for data collection. Diffraction data were collected on an Enraf-Nonius CAD4 diffractometer for **1** and a Rigaku 7S four-circle diffractometer for **2**, **3**, and **4**; the diffractometers were equipped with graphite monochromatized Mo Kα radiation ($\lambda$ = 0.710 69 Å). Empirical absorption corrections ($\psi$-scans) were carried out in each case. Three standard reflections were measured every 2 h for **1** and every 200 data collections for the others, and they revealed no fluctuation in intensities. The lattice constants were optimized from a least-squares refinement of the settings of 25 carefully centered Bragg reflections in the range of 25° < 2$\theta$ < 30°. The maximum and minimum transmission factors were 0.830 and 0.870 for **1**, 0.557 and 0.640 for **2**, 0.229 and 0.320 for **3**, and 0.278 and 0.503 for **4**.

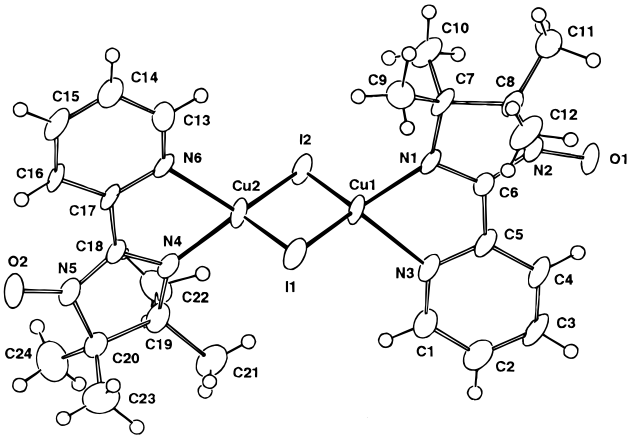


**Figure 1.** ORTEP drawing of $[Cu(\mu\text{-}I)(impy)]_2$ (**1**).

Crystallographic data are collected in Table 1. The structures were solved by the direct method with SHELX-86[13] and Fourier techniques and were refined by the full-matrix least-squares method using XTAL 3.2.[14] All non-hydrogen atoms were readily located and refined with anisotropic thermal parameters, and hydrogen atoms were located from difference Fourier maps and refined with isotropic thermal parameters. In **1**, the relatively large maximum peak (2.17 e Å$^{-3}$) was observed in the final difference Fourier syntheses. Because this peak locates close (1.1 Å) to the iodine ion, we ignored this peak. Convergence was reached at $R = 0.039$ and $R_w = 0.058$ (3497 reflections with $I > 3\sigma I$) for **1**, while these numbers were 0.025 and 0.033 (2223 reflections with $I > 3\sigma I$) for **2**, 0.027 and 0.032 (1766 reflections with $I > 1.5\sigma I$) for **3**, and 0.029 and 0.037 (2222 reflections with $I > 3\sigma I$) for **4**. Final atomic parameters and equivalent isotropic thermal parameters for non-hydrogen atoms are listed in Tables 2, 3, 4, and SXII.

**Molecular Orbital Calculations.** Molecular orbital calculations for the imino nitroxide ligands were carried out using the PM3 Hamiltonian and an RHF method in MOPAC, Ver. 6.00 (QCPE No. 445).[15]

## Results

**Description of Structure. (a) $[Cu(\mu\text{-}I)(impy)]_2$ (1).** The structure is noncentrosymmetric. The noncentrosymmetric structure and its inversion were refined using the complete data set of all observed reflections and 289 variable parameters. The final $R/R_w$ values for the structure presented here were calculated to be 0.039/0.058, and those for its inversion were calculated to be 0.040/0.060. An ORTEP drawing of the molecule is depicted in Figure 1, and selected intramolecular bond lengths and angles are listed in Table 5. The structure of the complex molecule consists of discrete dimers. In the dimer, two copper(I) ions are bridged by two iodide ions, where the bond angles between two copper and bridging iodide ions are close to 60°, and the metal centers are separated by 2.592(2) Å. Coordination geometry about the copper ion is a distorted tetrahedron with two nitrogen atoms of the impy and two iodide ions. The Cu−N(pyridine) distances (2.162(9)−2.171(9) Å) are longer than the Cu−N(imino nitroxide) distances (2.005(9)−2.007(9) Å), and the Cu−I distances are in the range of 2.571(2)−2.631(2) Å. In a noncoordinated radical species, such as *p*-pyridyl nitronyl nitroxide, the pyridine and nitronyl nitroxide planes tilt toward each other (22.8°).[16] Chelation of impy leads to coplanarity of the imino nitroxide fragments (N1−C6−N2−O1 and N4−C18−N5−O2) and the pyridine planes (the dihedral angles between two planes are 5.2(9)° and 3.2(9)°, respectively).

(10) (a) Ullman, E. F.; Call, L.; Osiecki, J. H. *J. Org. Chem.* **1970**, *35*, 3623. (b) Caneschi, A.; Gatteschi, D.; Rey, P. *Prog. Inorg. Chem.* **1991**, *39*, 331.
(11) Kubas, G. J.; Monzyk, B.; Crumbliss, A. L. *Inorg. Synth.* **1979**, *19*, 90.
(12) *Theory and Application of Molecualr Paramagnetism*; Boudreaux, E. A., Mulay, L. N., Eds.; Wiley and Sons, Inc.: New York, 1976.
(13) Sheldrick, G. M. *SHELXS-86*; University of Göttingen: Göttingen, Germany, **1986**.
(14) Hall, S. R.; Sterwart, J. M. *XTAL3.2*; Universities of Western Australia and Maryland: Nedlands, Australia, and College Park, MD, 1992.
(15) Stewart, J. J. *QCPE Bull.* **1990**, *10* (4), 86.
(16) Awaga, K.; Inabe, T.; Maruyama, Y. *Chem. Phys. Lett.* **1992**, *190*, 349.

**Table 1.** Crystallographic Data for $[Cu(\mu\text{-I})(impy)]_2$ (**1**), $[Cu(\mu\text{-I})(immepy)]_2$ (**2**), $[Cu(\mu\text{-Br})(immepy)]_2$ (**3**), and $[Cu(\mu\text{-Br})(imph\text{-}NO_2)]_2$ (**4**)

| | **1** | **2** | **3** | **4** |
|---|---|---|---|---|
| formula | $C_{24}H_{32}Cu_2I_2N_6O_2$ | $C_{26}H_{36}Cu_2I_2N_6O_2$ | $C_{26}H_{36}Cu_2Br_2N_6O_2$ | $C_{26}H_{32}Br_2Cu_2N_6O_6$ |
| formula weight | 817.46 | 845.51 | 751.51 | 811.48 |
| temperature (°C) | −100 | 20 | −120 | −120 |
| space group | $P2_12_12_1$ (No. 19) | $P2_1/c$ (No. 14) | $P2_1/c$ (No. 14) | $P2_1/c$ (No. 14) |
| $a$ (Å) | 17.807(2) | 9.941(2) | 9.964(6) | 11.991(7) |
| $b$ (Å) | 8.595(2) | 18.482(2) | 18.167(4) | 17.998(8) |
| $c$ (Å) | 19.336(6) | 8.337(2) | 8.009(7) | 7.215(6) |
| $\beta$ (deg) | | 96.41(2) | 95.81(6) | 104.07(6) |
| $V$ (Å3) | 2959(1) | 1522.2(6) | 1442(2) | 1510(2) |
| $Z$ | 4 | 2 | 2 | 2 |
| $\rho_{calc}$ (g cm$^{-3}$) | 1.84 | 1.84 | 1.73 | 1.78 |
| $\lambda$(Mo K$\alpha$) (Å) | 0.71069 | 0.71069 | 0.71069 | 0.71069 |
| $\mu$ (cm$^{-1}$) | 35.37 | 34.41 | 52.58 | 40.82 |
| $R$[a] | 0.039 | 0.025 | 0.027 | 0.029 |
| $R_w$[b] | 0.058 | 0.033 | 0.032 | 0.037 |

[a] $R = \sum(|F_o| - |F_c|)/\sum|F_o|$. [b] $R_w = [\sum w(|F_o| - |F_c|)^2/\sum w|F_o|^2]^{1/2}$; $w = (\sigma_c^2+(0.025|F_o|)^2)^{-1}$ for (**1**), $w = (\sigma_c^2+(0.015|F_o|)^2)^{-1}$ for (**2**), (**3**), and (**4**).

**Table 2.** Fractional Coordinates and Equivalent Isotropic Displacement Parameters (Å$^2$) of Non-Hydrogen Atoms of $[Cu(\mu\text{-I})(impy)]_2$ (**1**)

| | $x/a$ | $y/b$ | $z/c$ | $U$[a] |
|---|---|---|---|---|
| I(1) | 0.47882(4) | 1.18737(9) | 0.43847(5) | 0.0423(2) |
| I(2) | 0.49106(4) | 0.75818(8) | 0.57135(4) | 0.0389(2) |
| Cu(1) | 0.54622(7) | 0.9357(2) | 0.47474(8) | 0.0349(4) |
| Cu(2) | 0.42201(7) | 1.0101(2) | 0.53629(8) | 0.0357(4) |
| O(1) | 0.7679(4) | 0.690(1) | 0.3390(5) | 0.048(3) |
| O(2) | 0.2183(4) | 1.321(1) | 0.6689(5) | 0.052(3) |
| N(1) | 0.5950(4) | 0.819(1) | 0.3967(5) | 0.032(3) |
| N(2) | 0.6989(4) | 0.725(1) | 0.3473(5) | 0.032(3) |
| N(3) | 0.6639(5) | 0.961(1) | 0.5020(5) | 0.033(3) |
| N(4) | 0.3793(5) | 1.132(1) | 0.6155(5) | 0.031(3) |
| N(5) | 0.2834(5) | 1.263(1) | 0.6621(6) | 0.036(3) |
| N(6) | 0.3047(5) | 1.019(1) | 0.5077(5) | 0.031(3) |
| C(1) | 0.6956(7) | 1.039(2) | 0.5547(7) | 0.037(4) |
| C(2) | 0.7722(7) | 1.049(2) | 0.5607(8) | 0.048(5) |
| C(3) | 0.8189(7) | 0.971(2) | 0.5162(8) | 0.051(5) |
| C(4) | 0.7868(6) | 0.885(2) | 0.4649(7) | 0.038(4) |
| C(5) | 0.7096(6) | 0.885(1) | 0.4576(6) | 0.028(3) |
| C(6) | 0.6687(5) | 0.809(1) | 0.4004(6) | 0.026(3) |
| C(7) | 0.5692(5) | 0.727(1) | 0.3357(7) | 0.034(3) |
| C(8) | 0.6413(6) | 0.705(1) | 0.2922(7) | 0.035(3) |
| C(9) | 0.5057(7) | 0.813(2) | 0.2996(7) | 0.047(4) |
| C(10) | 0.5387(7) | 0.575(2) | 0.3632(8) | 0.045(4) |
| C(11) | 0.6512(8) | 0.550(2) | 0.2564(9) | 0.055(5) |
| C(12) | 0.6542(9) | 0.840(2) | 0.2408(9) | 0.057(6) |
| C(13) | 0.2697(7) | 0.959(1) | 0.4544(7) | 0.039(4) |
| C(14) | 0.1932(7) | 0.981(2) | 0.4417(8) | 0.045(4) |
| C(15) | 0.1530(7) | 1.073(2) | 0.4853(8) | 0.046(4) |
| C(16) | 0.1889(5) | 1.143(1) | 0.5417(7) | 0.034(3) |
| C(17) | 0.2645(5) | 1.112(1) | 0.5515(6) | 0.028(3) |
| C(18) | 0.3092(5) | 1.170(1) | 0.6094(6) | 0.027(3) |
| C(19) | 0.4059(6) | 1.184(2) | 0.6855(7) | 0.044(4) |
| C(20) | 0.3477(6) | 1.306(1) | 0.7079(7) | 0.036(4) |
| C(21) | 0.4859(8) | 1.240(2) | 0.6799(8) | 0.062(6) |
| C(22) | 0.4048(9) | 1.038(2) | 0.7318(7) | 0.048(5) |
| C(23) | 0.370(1) | 1.472(2) | 0.690(1) | 0.059(6) |
| C(24) | 0.323(1) | 1.300(3) | 0.7832(9) | 0.067(6) |

[a] Equivalent isotropic $U$ defined as one-third of the trace of the orthogonalized $\mathbf{U}_{ij}$ tensor.

**Table 3.** Fractional Coordinates and Equivalent Isotropic Displacement Parameters (Å$^2$) of Non-Hydrogen Atoms of $[Cu(\mu\text{-I})(immepy)]_2$ (**2**)

| | $x/a$ | $y/b$ | $z/c$ | $U$ |
|---|---|---|---|---|
| Cu | 0.43763(6) | 0.06239(3) | 0.45464(5) | 0.0396(2) |
| I | 0.61229(3) | 0.00371(1) | 0.28345(3) | 0.0423(1) |
| O(1) | 0.1286(5) | 0.2690(2) | 0.2001(3) | 0.068(1) |
| N(1) | 0.4782(3) | 0.1774(2) | 0.4845(3) | 0.031(1) |
| N(2) | 0.2704(3) | 0.1060(2) | 0.3290(3) | 0.031(1) |
| N(3) | 0.1548(4) | 0.2032(2) | 0.2337(3) | 0.040(1) |
| C(1) | 0.5823(5) | 0.2101(2) | 0.5716(4) | 0.037(1) |
| C(2) | 0.5894(5) | 0.2856(2) | 0.5814(4) | 0.045(1) |
| C(3) | 0.4920(5) | 0.3270(2) | 0.4944(4) | 0.047(1) |
| C(4) | 0.3870(5) | 0.2938(2) | 0.4023(4) | 0.040(1) |
| C(5) | 0.3822(4) | 0.2192(2) | 0.4037(4) | 0.031(1) |
| C(6) | 0.2709(4) | 0.1757(2) | 0.3209(3) | 0.031(1) |
| C(7) | 0.1474(4) | 0.0771(2) | 0.2306(4) | 0.033(1) |
| C(8) | 0.0516(5) | 0.1442(2) | 0.2069(4) | 0.039(1) |
| C(9) | 0.1945(6) | 0.0502(3) | 0.0746(5) | 0.049(2) |
| C(10) | 0.0917(7) | 0.0146(3) | 0.3202(5) | 0.049(2) |
| C(11) | −0.0412(7) | 0.1521(3) | 0.3399(5) | 0.059(2) |
| C(12) | −0.0279(7) | 0.1528(3) | 0.0419(6) | 0.061(2) |
| C(13) | 0.6883(7) | 0.1622(3) | 0.6557(5) | 0.054(2) |

**Table 4.** Fractional Coordinates and Equivalent Isotropic Displacement Parameters (Å$^2$) of Non-Hydrogen Atoms of $[Cu(\mu\text{-Br})(imph\text{-}NO_2)]_2$ (**4**)

| | $x/a$ | $y/b$ | $z/c$ | $U$ |
|---|---|---|---|---|
| Br | 0.09711(5) | 0.47354(2) | 0.34486(3) | 0.0241(1) |
| Cu | 0.07303(6) | 0.45639(3) | 0.66979(4) | 0.0235(2) |
| O(1) | 0.2568(4) | 0.2713(2) | 1.2191(3) | 0.037(1) |
| O(2) | −0.3415(5) | 0.2355(2) | 0.9803(3) | 0.039(1) |
| O(3) | −0.2776(5) | 0.1366(2) | 0.8737(3) | 0.039(1) |
| N(1) | 0.1769(4) | 0.4029(2) | 0.8687(2) | 0.0171(9) |
| N(2) | 0.2542(4) | 0.3236(2) | 1.0992(3) | 0.022(1) |
| N(3) | −0.2675(5) | 0.2012(2) | 0.9266(3) | 0.026(1) |
| C(1) | 0.1573(5) | 0.3466(2) | 0.9672(3) | 0.016(1) |
| C(2) | 0.3008(5) | 0.4240(2) | 0.9286(3) | 0.019(1) |
| C(3) | 0.3564(5) | 0.3694(2) | 1.0954(3) | 0.020(1) |
| C(4) | 0.3502(6) | 0.4167(3) | 0.7541(4) | 0.032(2) |
| C(5) | 0.3049(7) | 0.5058(2) | 0.9893(4) | 0.032(1) |
| C(6) | 0.4491(6) | 0.3185(2) | 1.0581(4) | 0.025(1) |
| C(7) | 0.3990(6) | 0.4047(3) | 1.2912(4) | 0.029(1) |
| C(8) | 0.0459(5) | 0.3090(2) | 0.9501(3) | 0.016(1) |
| C(9) | −0.0517(5) | 0.3507(2) | 0.9483(3) | 0.019(1) |
| C(10) | −0.1547(5) | 0.3156(2) | 0.9405(3) | 0.021(1) |
| C(11) | −0.1586(5) | 0.2392(2) | 0.9317(3) | 0.018(1) |
| C(12) | −0.0641(5) | 0.1971(2) | 0.9273(3) | 0.021(1) |
| C(13) | 0.0396(5) | 0.2319(2) | 0.9394(3) | 0.020(1) |

Coordinating ligands in the adjacent molecules are stacked to form a one-dimensional chain along the [101] direction, and the chains are linked by $CuI_2Cu$ units, which leads to the formation of the two-dimensional network. Figure 3a shows the stacking arrangements in views parallel and perpendicular to the imino nitroxide fragments. Within the stack, the adjacent radical ligands are related by ($^1/_2 + x$, $^1/_2 - y$, $1 - z$) and the N−O groups are close to each other (O1···N4′ = 3.52(1) Å). It should be noted that the closest intermolecular distance is observed between the oxygen atom (O1) of the nitroxide and the sp$^2$ carbon atom of the next imino nitroxide moiety (O1···C18′ = 3.33(1) Å). The conjugated imino−nitroxyl fragments of the two adjacent molecules (O1−N2−C6−N1 and O2′−N5′−C18′−N4′) make an angle of 22.0(8)°.

**Table 5.** Selected Bond Distances (Å) and Angles (deg) of $[Cu(\mu\text{-}I)(impy)]_2$ (**1**)

| | | | |
|---|---|---|---|
| I1−Cu1 | 2.571(2) | I1−Cu2 | 2.631(2) |
| I2−Cu1 | 2.604(2) | I2−Cu2 | 2.581(2) |
| Cu1−N1 | 2.007(9) | Cu1−N3 | 2.171(9) |
| Cu2−N4 | 2.005(9) | Cu2−N6 | 2.162(9) |
| Cu1−Cu2 | 2.592(2) | | |
| O1−N2 | 1.27(1) | O2−N5 | 1.27(1) |
| N1−C6 | 1.32(1) | N2−C6 | 1.36(1) |
| N4−C18 | 1.30(1) | N5−C18 | 1.37(1) |
| Cu1−I1−Cu2 | 59.75(5) | Cu1−I2−Cu2 | 59.98(5) |
| I1−Cu1−I2 | 120.83(6) | I1−Cu1−Cu2 | 61.27(5) |
| I2−Cu2−Cu1 | 60.47(5) | I2−Cu1−Cu2 | 59.56(5) |
| I1−Cu2−Cu1 | 58.97(5) | I1−Cu1−N1 | 114.6(3) |
| I1−Cu1−N3 | 115.6(2) | I2−Cu1−N1 | 114.2(3) |
| I2−Cu1−N3 | 104.4(3) | N1−Cu1−N3 | 79.3(3) |
| I1−Cu2−I2 | 119.44(6) | I1−Cu2−N4 | 113.1(3) |
| I1−Cu2−N6 | 99.7(3) | I2−Cu2−N4 | 114.7(3) |
| I2−Cu2−N6 | 123.8(3) | N4−Cu2−N6 | 79.1(4) |
| Cu1−N1−C6 | 115.2(7) | Cu1−N1−C7 | 136.4(6) |
| Cu1−N3−C1 | 129.7(8) | Cu1−N3−C5 | 112.3(7) |
| Cu2−N4−C18 | 115.3(8) | Cu2−N4−C19 | 136.5(7) |
| Cu2−N6−C13 | 130.3(8) | Cu2−N6−C17 | 111.6(7) |

**Table 6.** Intramolecular Bond Distances (Å) and Angles (deg) of $[Cu(\mu\text{-}I)(immepy)]_2$ (**2**)

| | | | |
|---|---|---|---|
| Cu−I | 2.6041(7) | Cu−I* | 2.5978(7) |
| Cu−N1 | 2.173(3) | Cu−N2 | 2.030(3) |
| Cu−Cu* [a] | 2.6869(8) | | |
| O1−N3 | 1.269(4) | N2−C6 | 1.290(5) |
| N3−C6 | 1.390(4) | | |
| I−Cu−Cu* | 58.79(2) | I−Cu−I* | 117.80(2) |
| Cu−Cu*−I | 59.02(2) | Cu−I−Cu* | 62.20(2) |
| I−Cu−N1 | 110.10(8) | I−Cu−N2 | 116.10(9) |
| N1−Cu−N2 | 78.6(1) | N1−Cu−I | 114.47(8) |
| N2−Cu−I | 113.46(9) | Cu−N1−C1 | 128.7(2) |
| Cu−N1−C5 | 113.0(2) | Cu−N2−C6 | 114.5(2) |
| Cu−N2−C7 | 135.7(2) | | |

[a] Key to symmetry operation *: $1 - x, -y, 1 - z$.

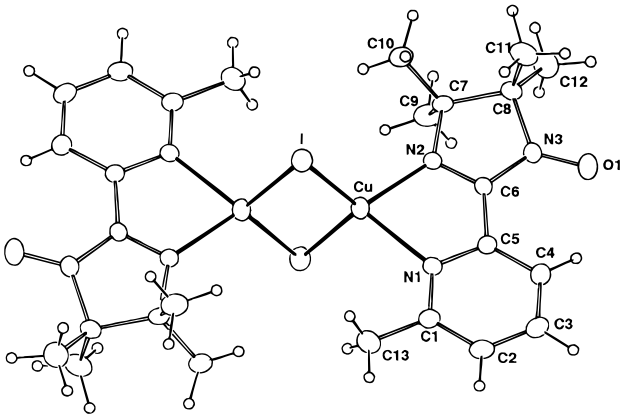


**Figure 2.** ORTEP drawing of $[Cu(\mu\text{-}I)(immepy)]_2$ (**2**).

**(b) $[Cu(\mu\text{-}I)(immepy)]_2$ (2).** An ORTEP drawing of **2** is depicted in Figure 2. Selected intramolecular bond distances and angles are listed in Table 6. Complex **2** crystallizes in the monoclinic space group $P2_1/c$. The complex molecule has a halogen-bridged dinuclear form and is positioned on a crystallographic inversion center. Copper ions in each asymmetric unit are bridged by the two iodide ions, and the two copper ions in the molecule are separated by 2.6869(8) Å. Coordination geometry about the copper ion is a pseudotetrahedron, and the four coordination sites are completed by the two nitrogen atoms from immepy and two bridging iodide ions. Bond distances about the copper ion are similar to those of **1**. The Cu−N(imino nitroxide) bond is shorter (2.030(3) Å) than the Cu−N(pyridine) bond (2.173(3) Å), and the Cu−I bond distances are 2.5978(7)−2.6041(7) Å. The imino nitroxide fragment and the pyridine ring in the molecule make an angle of 5.9(5)°. Complex molecules are aligned in the [101] direction, and the radicals are stacked with close inter-radical distances (O1···N3′ = 3.968(7) Å and O1···C6′ = 3.751(8) Å) (Figure 3b). The dihedral angle formed by the conjugated imino−nitroxyl fragments of two adjacent molecules (O1−N3−C6−N2 and O1′−N3′−C6′−N2′) is only 6.8(4)°.

**Table 7.** Intramolecular Bond Distances (Å) and Angles (deg) of $[Cu(\mu\text{-}Br)(immepy)]_2$ (**3**)

| | | | |
|---|---|---|---|
| Cu−Br | 2.4439(5) | Cu−Br* | 2.4424(5) |
| Cu−N1 | 2.163(3) | Cu−N2 | 1.996(2) |
| Cu−Cu* | 2.7357(6) | | |
| O1−N3 | 1.266(3) | N2−C6 | 1.299(4) |
| N3−C6 | 1.381(4) | | |
| Br−Cu−Cu* [a] | 55.93(1) | Br−Cu−Br* | 111.91(2) |
| Cu−Cu*−Br* | 55.98(1) | Cu−Br−Cu* | 68.09(2) |
| Br−Cu−N1 | 117.08(6) | Br−Cu−N2 | 115.44(7) |
| N1−Cu−N2 | 79.11(9) | N1−Cu−Br | 111.20(7) |
| N2−Cu−Br | 118.47(7) | Cu−N1−C1 | 129.4(2) |
| Cu−N1−C5 | 112.8(2) | C1−N1−C5 | 117.9(3) |
| Cu−N2−C6 | 115.3(2) | Cu−N2−C7 | 135.3(2) |

[a] Key to symmetry operation *: $1 - x, -y, 1 - z$.

**Table 8.** Intramolecular Bond Lengths (Å) and Angles (deg) of $[Cu(\mu\text{-}Br)(imph\text{-}NO_2)]_2$ (**4**)

| | | | |
|---|---|---|---|
| Br−Cu | 2.450(2) | Br*−Cu[a] | 2.379(1) |
| Cu−N1 | 1.915(3) | Cu−Cu* | 3.074(2) |
| O1−N2 | 1.274(4) | N1−C1 | 1.291(5) |
| N2−C1 | 1.375(4) | | |
| Cu−Br−Cu | 79.05(3) | Br−Cu−Cu | 49.45(4) |
| Br−Cu−Br | 100.95(3) | Br−Cu−Cu | 51.50(3) |
| Br−Cu−N1 | 125.0(1) | N1−Cu−Br | 134.0(1) |
| Cu−N1−C1 | 129.4(2) | Cu−N1−C2 | 120.6(2) |

[a] Key to symmetry operation *: $-x, 1 - y, 1 - z$.

**(c) $[Cu(\mu\text{-}Br)(immepy)]_2$ (3).** Crystals of **3** and **2** are isomorphous. The atomic numbering system in **3** is the same as that used in **2** except for the iodide ion. Selected intramolecular bond distances and angles are listed in Table 7. The structure consists of discrete dimer, and in this dimeric entity two copper ions are bridged by two bromide ions. Owing to the geometrical configuration, there is a inversion center in the middle of the Cu−Cu vector. Coordination geometry of the copper ion is a distorted tetrahedron. The Cu−N(pyridine) and Cu−N(imino nitroxide) distances are 2.164(3) and 1.996(2) Å, respectively, and the corresponding distances of the two Cu−Br bonds are 2.443(1) and 2.444(2) Å. The imino nitroxide fragment and the pyridine ring in the molecule are almost coplanar (the dihedral angle between them is 1.4(1)°). The two copper and one bridging bromide ions make a distorted equilateral triangle with a Cu···Cu distance of 2.7360(8) Å. The radicals immepy are stacked in the same manner as in **2**, where the intermolecular O1···N3′ and O1···C6′ distances within the stacks are 3.774(7) and 3.588(7) Å, respectively. The dihedral angle between the conjugated imino−nitroxyl fragments of two adjacent molecules (O1−N3−C6−N2 and O1′−N3′−C6′−N2′) is 8.3(4)°.

**(d) $[Cu(\mu\text{-}Br)(imph\text{-}NO_2)]_2$ (4).** Complex **4** forms a halogen-bridged dinuclear molecule which has an inversion center in the middle of copper ions. An ORTEP diagram with numbering schemes is depicted in Figure 4. Selected intramolecular bond distances and angles are listed in Table 8. The coordination geometry about the copper ions is a triangle, where the copper ion is displaced 0.035(2) Å from the mean plane defined by N1, Br, and Br′ atoms. The Cu−N(imino nitroxide) bond

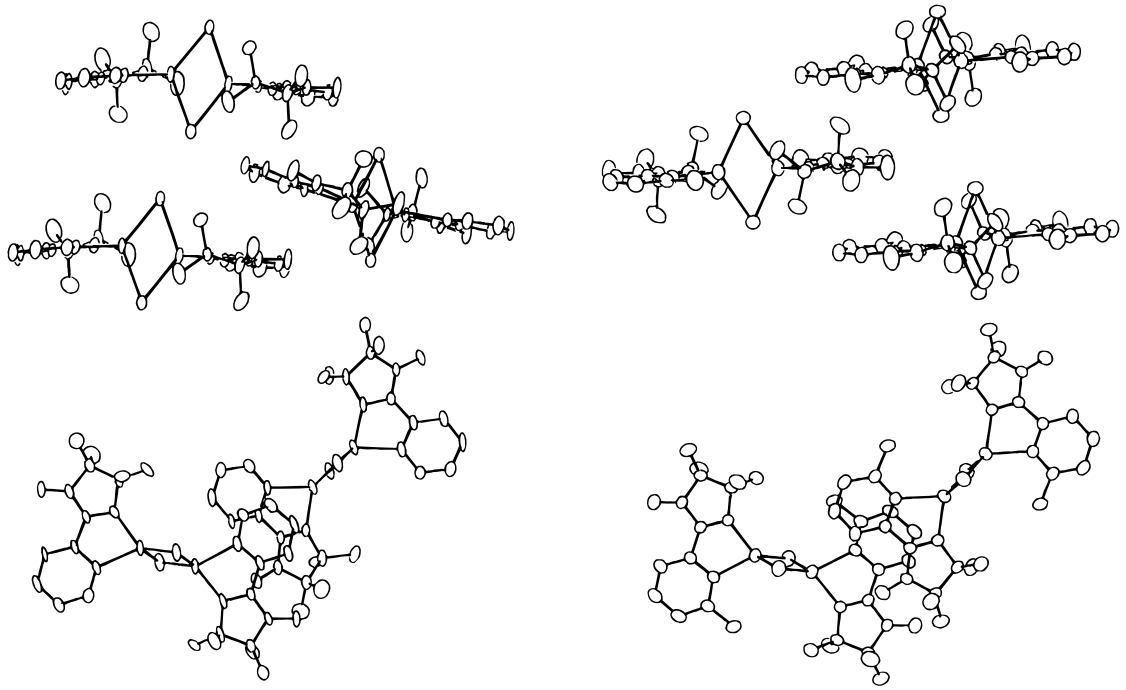


**Figure 3.** Packing diagram in a view parallel and perpendicular to the imino nitroxides of (a) [Cu($\mu$-I)(impy)]$_2$ (**1**) and (b) [Cu($\mu$-I)(immepy)]$_2$ (**2**).

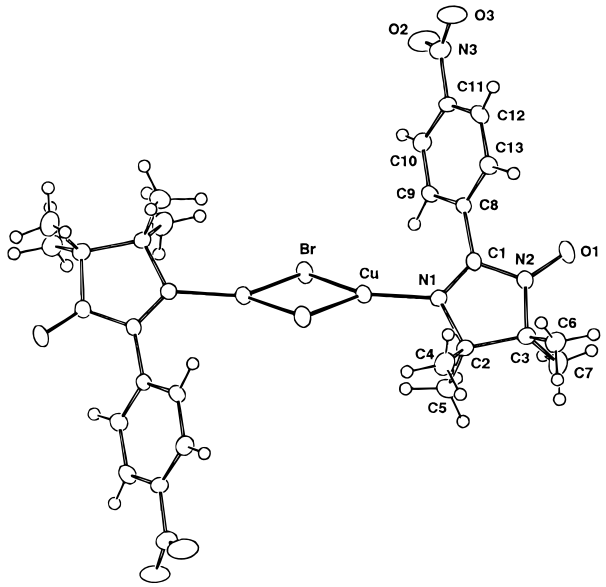


**Figure 4.** ORTEP drawing of [Cu($\mu$-Br)(imph-NO$_2$)]$_2$ (**4**).

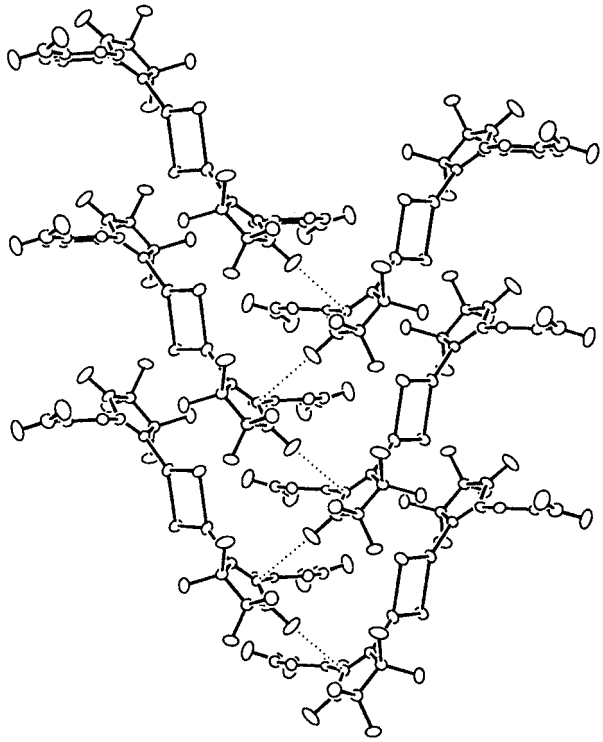

**Figure 5.** Chain structure of [Cu($\mu$-Br)(imph-NO$_2$)]$_2$ (**4**).

distance is 1.915(3) Å, which is slightly shorter than the corresponding bond distances (1.996(2)−2.030(3) Å) for **1**−**3**. The imino−nitroxyl fragment (N1−C1−N2−O1) makes an angle of 58.2(5) ° with a Cu−Br−Br′ plane. The intramolecular Cu···Cu distance across bromide bridges is 3.074(2) Å. The coordinating imino nitroxides form a chain structure (Figure 5), where the adjacent imino nitroxides are related by ($-x$, $y + {}^1/_2$, $-z + {}^1/_2$). In the chain the oxygen atom of the N−O group is directed toward the sp$^2$ carbon atom of the neighboring imino nitroxide moiety with the interatomic distance (O1···C1′) of 3.188(5) Å. It should be noted that the dihedral angle of the adjacent imino−nitroxyl fragments is 101.2(4)°.

**Magnetic Properties.** Temperature dependent magnetic susceptibilities for **1**−**4** have been measured down to 2.0 K. $\chi_m T$ values vs $T$ (temperature) plots for **1**−**3** are depicted in Figure 6, and both $\chi_m T$ values vs $T$ and $\chi_m$ values vs $T$ plots for **4** are depicted in Figure 7, where $\chi_m$ is molar magnetic susceptibility.

For **1**−**4**, the $\chi_m T$ values (0.70−0.73 emu mol$^{-1}$ K) at 300 K are smaller than the values expected for uncorrelated spins (0.75 emu mol$^{-1}$ K), which is due to the small diamagnetic impurities like copper halides. On lowering the temperature, $\chi_m T$ for **1** increases and exhibits a maximum at 16 K ($\chi_m T$ = 0.80 emu mol$^{-1}$ K) and then decreases, while constant decreases down to 2 K are observed in **2**, **3**, and **4**. These magnetic behaviors suggest that in **1** some ferromagnetic interaction is predominant at intermediate temperatures and then a weaker

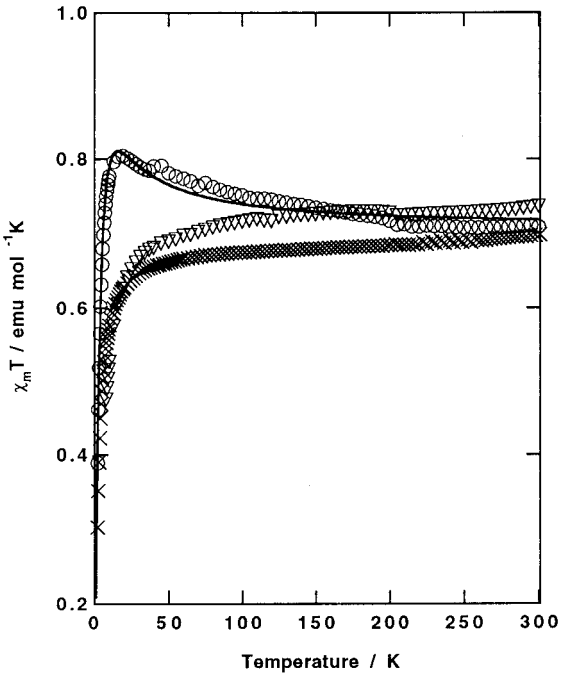


**Figure 6.** Experimental and calculated (—) $\chi_m T$ *vs* $T$ plots for [Cu($\mu$-I)(impy)]$_2$ (**1**) (○), [Cu($\mu$-I)(immepy)]$_2$ (**2**) (×), and [Cu($\mu$-Br)(immepy)]$_2$ (**3**) (▽).

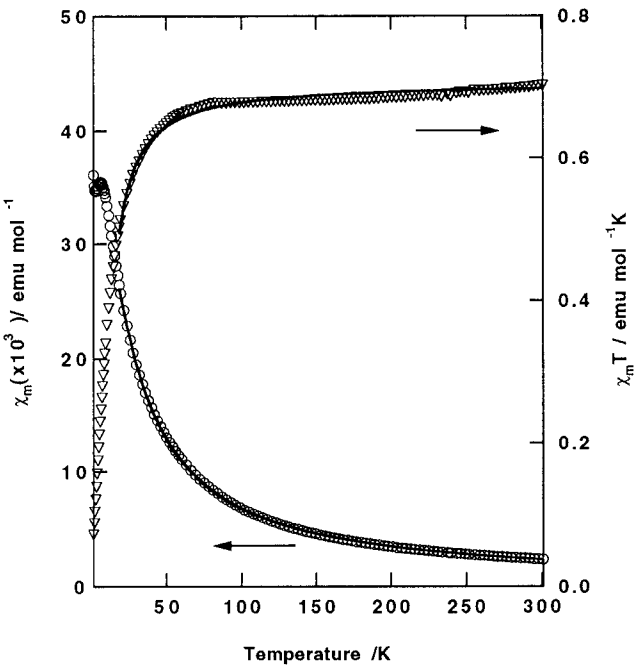


**Figure 7.** Plots of $\chi_m T$ (▽) and $\chi_m$ (○) *vs* $T$ for [Cu($\mu$-Br)(imph-NO$_2$)]$_2$ (**4**). Solid lines correspond to the best fitted curves by using the data above 20 K.

antiferromagnetic coupling is involved at lower temperature, while in **2** and **3** radicals are antiferromagnetically coupled.

The structural analysis of **1** shows that the radical ligands are stacked to form a chain with the short contact (O1···N4′ = 3.52(1) and O1···C18′ = 3.33(1) Å), while the Cu−I$_2$−Cu unit separates the coordinating radicals by 6.33(1) Å (= N1···N4). Therefore, the magnetic interaction in **1** can be interpreted as a ferromagnetic intrachain interaction with a weak interchain (intramolecular) antiferromagnetic interaction. Assuming isotropic Heisenberg interaction, the Hamiltonian is expressed as

$$H = -2J\sum S_i S_{i+1} \qquad (1)$$

where $J$ is the intrachain-exchange coupling constant and the summation is over all members of the chain. The magnetic susceptibility for the Heisenberg ferromagnetic chain can be expressed by the equation based on the high-temperature Padé expansion by Bakers et al.[17] as

$$\chi_m = Ng^2\mu_B{}^2\left[\frac{1 + a_1K + a_2K^2 + a_3K^3 + a_4K^4 + a_5K^5}{1 + b_1K + b_2K^2 + b_3K^3 + b_4K^4}\right] \qquad (2)$$

where $K = J_F/2k_BT$ and $a_i$ and $b_i$ are expansion coefficients. $N$, $g$, $\mu_B$, and $K_B$ are Avogadro's number, $g$ factor, Bohr magneton, and Boltzmann constant, respectively. The total magnetic susceptibility is

$$\chi'_m = \frac{\chi_m}{[1 - 2zJ'\chi_m/Ng^2\mu_B{}^2]} \qquad (3)$$

where $J'$ and $z$ are the interchain interaction and the number of neighboring chains, respectively. The least-squares fitting of the experimental data with eq 3 led to $J_F = 5.8(2)$ cm$^{-1}$, $J' = -2.2(1)$ cm$^{-1}$ ($z = 2$), and $g = 1.94(1)$ for **1**.

The magnetic behaviors of **2** and **3** are different from that of **1** in spite of the fact that the radicals are aligned in the chain structure. In **2** and **3** gradual decrease in $\chi_m T$ values down to 2.0 K suggest that both intra- and interchain antiferromagnetic interactions are operative. The X-ray structural analyses for **2** and **3** revealed the equidistant stacks of the radicals; therefore, the magnetic data can be interpreted by Bonner and Fisher's equation.[18] Total magnetic susceptibility can be expressed as eq 3 which includes interchain interaction. The best fits to the data were obtained with $J_{AF} = -0.68(2)$ cm$^{-1}$, $J' = -0.40(4)$ cm$^{-1}$ ($z = 2$), and $g = 1.91(1)$ for **2**, and $J_{AF} = -1.12(2)$ cm$^{-1}$, $J' = -0.25(5)$ cm$^{-1}$ ($z = 2$), and $g = 2.00(1)$ for **3**. The amplitudes of the interchain interactions are comparable to those of intrachain interactions; therefore, the magnetic susceptiblity data for **2** and **3** were analyzed by the Curie−Weiss equation. Curie and Weiss constants were estimated to be 0.70(1) emu mol$^{-1}$ K$^{-1}$ and −3.3(1) K for **2**, and 0.75(1) emu mol$^{-1}$ K$^{-1}$ and −1.16 K for **3**, respectively. It is concluded that both intra- and interchain magnetic interactions are antiferromagnetic.

In **4**, $\chi_m T$ values decrease as the temperature is lowered, which might lead to the conclusion of both inter- and intramolecular magnetic interactions being antiferromagnetic. However, the structural analysis, especially the stacking mode of the radicals, strongly supports that the intrachain magnetic interaction is ferromagnetic, and this will be discussed in detail. The magnetic susceptibility for **4** was, therefore, analyzed by the Heisenberg ferromagnetic chain model with an interchain (intramolecular) antiferromagnetic interaction ($zJ'$). Fitting eqs 2 and 3 to the experimental data yielded the following best fit parameters: $g = 1.91(1)$, $J_F$, = 13.4(4) cm$^{-1}$, and $J' = -11.4(2)$ cm$^{-1}$ ($z = 2$) for **4**, and the interchain interaction, that is, the intradimer interaction, appears to be rather large. Therefore, it is appropriate that the system is treated as a dimeric unit with an interdimer interaction. Thus

$$\chi_{dimer} = \frac{2Ng^2\mu_B{}^2}{3kT}\left[\frac{3}{3 + \exp(-2J_1/kT)}\right]$$

$$\chi_{total} = \chi_{dimer}T/(T - \theta)$$

with $\theta = 2zJ_2/3k$, z = 2, and $J_1$ and $J_2$ being intra- and

(17) Baker, G. A.; Rushbrooke, G. S.; Gilbert, H. E. *Phys. Rev.* **1964**, *135*, A1272.

(18) Bonner, J. C.; Fisher, M. E. *Phys. Rev.* **1964**, *135*, A640.

interdimer exchange interactions, respectively. The solid line in Figure 7 is for $g = 1.94(1)$, $J_1 = -8.7(3)$ cm$^{-1}$, and $\theta = 2.8(4)$ K. Only data for $T > 20$ K were included in the fit, since the mean field expression is only valid for $T \gg \theta$. The value of $\theta$ corresponds to $J_2 = 1.5$ cm$^{-1}$. The $|J|/|J'|$ and $|J_1|/|J_2|$ values for **1** and **4** are 2.6 and 5.8, respectively, which might not satisfy the requirement of the mean field correction. We do not attach any particular meaning to those fits, except that they give some support to the hypothesis of the ferromagnetic intrachain interactions for **1** and **4** and the substantial antiferromagnetic intradimer interaction in **4**.

## Discussion

Nitronyl nitroxides and imino nitroxides have been reported to have a variety of intermolecular magnetic couplings. Intermolecular ferromagnetic interactions have been observed in a series of nitroxides,[19] and some of them exhibit spontaneous magnetization at very low temperature (0.6 K).[20] In contrast to the ferromagnetic couplings, a large number of intermolecular antiferromagnetic couplings have been reported. The sign and magnitude of the intermolecular magnetic interactions depend strongly on a relative arrangement of adjacent N−O groups, and the correlation between the magnetic interactions and geometrical parameters has been discussed.[21] The magnetic interaction between two unpaired electrons is generally antiferromagnetic. The ferromagnetic interactions require that peculiar conditions are fulfilled. This situation has been well rationalized by Kahn et al.[22] and Miller and Epstein.[23] The conditions are (i) orthogonality of magnetic orbitals, (ii) spin polarization[24] (McConnell mechanism[25]), and (iii) ferromagnetic interaction involving charge transfer interactions (a configurational mixing interaction between ground and excited high-spin configurations).[26,27] This mechanism has been invoked to justify the ferromagnetic interactions in the ($\mu$-oxo)-bis($\mu$-acetato)-dimanganese complex,[28] [$Ln_2Cu_4$] hexanuclear cluster,[29] and *p*-nitrophenyl nitroxide.[20a]

Complex **1** shows intermolecular ferromagnetic coupling, while **2** and **3** show intermolecular antiferromagnetic interactions. Subtle differences in stacking modes must be responsible for magnetic behaviors in **1**−**3**. The spin density distributions in some nitronyl nitroxides have been determined by polarized neutron diffraction studies and MO calculations.[30] The positive spins are populated over the N−O groups, while the large negative spin density appears on the sp$^2$ carbon atom bridging two N−O groups. This indicates large spin-polarization effects on the nitronyl nitroxide. The electronic structures of pyridyl imino nitroxides are considered to be very similar to those of the nitronyl nitroxides. The positive spin density locates on both the imino-nitrogen atom and the N−O group, while the negative spin locates on the carbon atom. Structural analysis reveals that a short intermolecular contact in **1** involves the oxygen atom of the N−O group and the sp$^2$ carbon atom of the adjacent molecule (O1···C18′ = 3.33(1) Å) . The corresponding intermolecular contacts (O1···C6′) in **2** and **3** are 3.751(8) and 3.588(7) Å, respectively. These two atoms carry the opposite sign of the spin which alternates along the stack, and this matches McConnell's criteria. The observed contact distances in **1**−**3** suggest that the spin polarization leading to the intermolecular ferromagnetic interaction is more effective for **1** than for **2** and **3**. In addition to the imino−nitroxyl contacts, another significant intermolecular overlap is found between the conjugated imino−nitroxyl fragments (N−C−N−O) and the pyridine ring (Figure 3). PM3 MO calculations of the ligand impy with the coplanar arrangement of the imino nitroxide and the pyridine ring revealed that the SOMO (singly occupied molecular orbital) is mainly localized on the imino−nitroxyl moiety, while the LUMO (lowest unoccupied molecular orbital) is distributed on the whole $\pi$-conjugated system (Chart 2).

**Chart 2**

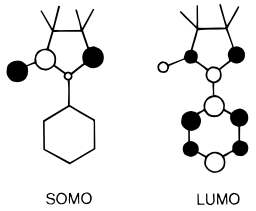


Intermolecular close contact of the N−C−N−O group and the pyridine rings in **1**−**3** implies SOMO−LUMO overlap, which leads to the intermolecular ferromagnetic interaction (the configurational mixing of high-spin ground and charge transfer configurations).[20a] In **2** and **3** the conjugated imino−nitroxyl fragments of two adjacent molecules stack with a parallel alignment, where dihedral angles between the two imino−nitroxyl planes are 6.8(4) and 8.3(4)°, respectively. In **1**, on the other hand, two imino−nitroxyl planes tilt toward each other with an angle of 22.0(8)°. Gatteschi and Rey have pointed out that a $\sigma$-type overlap (SOMO−SOMO overlap) of the nitronyl nitroxide $\pi^*$ orbital leads to the antiferromagnetic interaction, and this will be maximum when the adjacent N−O groups are parallel.[21] The resulting overlap in **2** and **3** favors the antiferromagnetic interaction, while the tilted stacking in **1** diminishes the antiferromagnetic contribution. As a result, in spite of the fact that the intermolecular short contacts in **1**−**3** contribute to the stabilization of the intermolecular ferromagnetic interaction due to the spin polarization and SOMO−LUMO overlaps, the intrachain magnetic interaction for **1** is ferromagnetic and those for **2** and **3** are antiferromagnetic.

Magnetic susceptibility measurements of **4** have shown that $\chi_m T$ values decrease as the temperature is lowered, that is, antiferromagnetic behavior. However, particular attention

(19) (a) Awaga, K; Inabe, T; Nagashilma, U; Maruyama, Y. *J. Chem. Soc., Chem. Commun*. **1989**, 1617. (b) Awaga, K.; Inabe, T.; Maruyama, Y. *Chem. Phys. Lett*. **1992**, *190*, 349. (c) Awaga, K.; Inabe, T.; Maruyama, Y. *Chem. Phys. Lett*. **1992**, *195*, 21.
(20) (a) Turek, P.; Nozawa, K.; Shiomi, D.; Awaga, K.; Inabe, T.; Maruyama, Y.; Kinoshita, M. *Chem. Phys. Lett*. **1991**, *180*, 327. (b) Takahashi, M.; Turek, P.; Nakazawa, Y.; Tamura, M.; Nozawa, K.; Shiomi, D.; Ishikawa, M.; Kinoshita, M. *Phys. Rev. Lett.* **1991**, *67*, 746.
(21) (a) Caneschi, A.; Ferrara, F.; Gatteschi, D.; Rey, P.; Sessoli, R. *Inorg. Chem*. **1990**, *29*, 1756. (b) Panthou, F. L.; Luneau, D.; Laugier, J.; Rey, P. *J. Am. Chem. Soc*. **1993**, *115*, 9095.
(22) Kollmar, C.; Kahn, O. *Acc. Chem. Res*. **1993**, *26*, 259.
(23) Miller, J. S.; Epstein, A. J. *Angew. Chem., Int. Ed. Engl*. **1994**, *33*, 385.
(24) (a) Izuoka, A.; Murata, S.; Sugawara, T.; Iwamura, H. *J. Am. Chem. Soc*. **1985**, *107*, 1786. (b) Izuoka, A.; Murata, S.; Sugawara, T.; Iwamura, H. *J. Am. Chem. Soc*. **1987**, *109*, 1631.
(25) McConnel, H. M. *J. Chem. Phys*. **1963**, *39*, 1910.
(26) McConnel, H. M. *Proc. Robert A. Welch Found. Conf. Chem. Res*. **1967**, *11*, 144.
(27) Goodenough, J. B. *Magnetism and the Chemical Bond*; Interscience Publishers: New York, 1963, 167.
(28) Hotzelmann, R.; Wieghardt, K.; Flörke, U.; Haupt, H.-J; Weatherburn, D. C.; Bonvoisin, J.; Blondin, G.; Girerd, J.-J. *J. Am. Chem. Soc*. **1992**, *114*, 1681.
(29) Andruh, M.; Ramade, I.; Codjovi, E.; Guillow, O.; Kahn, O.; Trombe, J. C. *J. Am. Chem. Soc*. **1993**, *115*, 1822.
(30) (a) Zheludev, A.; Barone, V.; Bonnet, M.; Delley, B.; Grand, A.; Ressouche, E.; Rey, P.; Subra, R.; Schweizer, J. *J. Am. Chem. Soc*. **1994**, 116, 2019. (b) Yamaguchi, K.; Okumura, M.; Maki, J.; Noro, T.; Namimoto, H.; Nakano, M.; Fueno, T. *Chem. Phys. Lett.* **1992**, *190*, 353. (c) Yamaguchi, K.; Okumura, M.; Nakano, M. *Chem. Phys. Lett*. **1992**, *191*, 237.

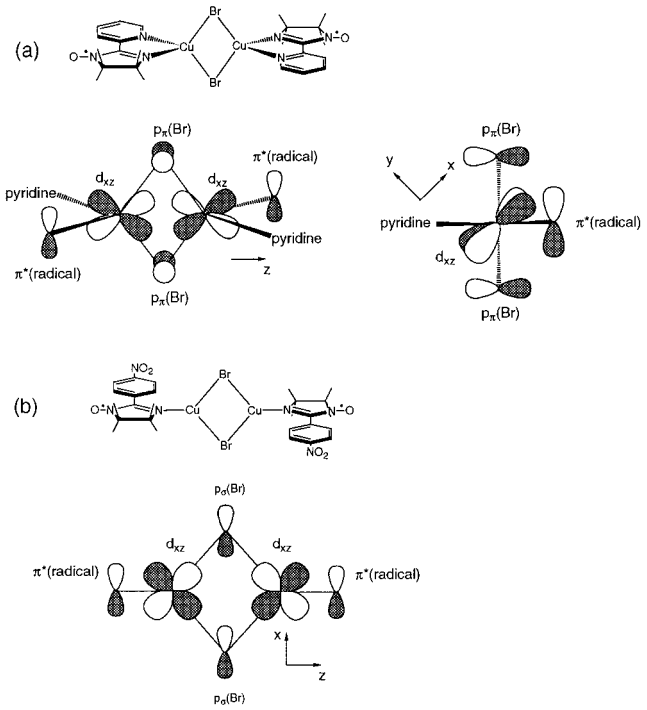


**Figure 8.** Orbital overlaps in (a) $[Cu(\mu\text{-}Br)(impy)]_2$ (along the *z*-axis (left) and perpendicular (right) to the *xy* plane), where the orbital overlaps with the $d_{yz}$ orbitals are omitted for clarity, and (b) $[Cu(\mu\text{-}Br)(imph\text{-}NO_2)]_2$ (pependicular to the *xz*-plane), where the radical $\pi^*$ orbital makes an angle of 31.8° with *xz*-plane.

should be given to the interpretation of the magnetic behavior for **4**. The structural analysis of **4** reveals that the stacking mode of the adjacent imino−nitroxyl groups is characteristic of the ferromagnetic interaction. In **4** the shortest interatomic contact (O1···C1′ = 3.188(5) Å) between adjacent imino nitroxides is observed among the complexes studied. Furthermore, the dihedral angle between adjacent imino nitroxides is 101.2(3)°. These fulfill the condition for the intrastack ferromagnetic interaction. A moderate intrastack ferromagnetic interaction ($J = 18$ cm$^{-1}$) was also observed for the imino nitroxide analog whose corresponding intermolecular contact and dihedral angles are 2.92 Å and 48.5°, respectively.[21b] If the intrastack ferromagnetic interaction is operative for **4**, a substantial intramolecular (intradimer) antiferromagnetic interaction must be propagated through a $Cu-Br_2-Cu$ bridge, and this intramolecular exchange interaction can be interpreted by the orbital topology of the fragments forming the dinuclear unit, that is, the triangular coordination geometry of **4**.

In the Cu(I)−diimine system $[Cu^I(TET)](ClO_4)$ (TET = 2,2′-bis(6-(2,2′-bipyridyl)biphenyl),[31] a $\pi$-back-donation of the copper $d_\pi$ electrons to the vacant ligand $\pi^*$ orbital has been confirmed by the electronic spectra. It is, therefore, expected that the overlap of SOMOs with metal $d_\pi$ orbitals induces substantial spin density on the $d_\pi$ orbital. In a tetrahedral coordination geometry like that of the copper ions in **1**−**3**, ligand $\pi^*$ orbitals (radical SOMOs) overlap with $d\pi$ ($d_{xz}$ and $d_{yz}$) orbitals,[33] which have a $\pi$-type overlap with $p_\pi$ orbitals of the bromide ions (Figure 8a). Magnetic orbitals on the radical ligands overlap with each other through the $d\pi(Cu)-Br(p\pi)-d\pi(Cu)$ orbitals ($\pi$-type pathway). On the other hand, the copper ions in **4** have a triangular coordination geometry, and the conjugated imino−nitroxyl fragment (N1−C1−N2−O1) makes an angle of 58.2(5)° with the $Cu-Br_2-Cu$ plane. As a result, the SOMOs ($\pi^*$) of the radical ligands tilt 31.8° toward the copper $d_{xz}$ orbitals, which makes the $d_{xz}$ and SOMO overlap possible. It can be also expected that the spin on the radicals is delocalized on the $d_{xz}$ orbital by this $\pi$-type overlap (by the $\pi$-back-donation). The triangular coordination of the copper ions, where the bond angle of Cu−Br−Cu is 79.05(3)°, compels the $d_{xz}$ orbital to have a $\sigma$-type overlap with $p_x$ (or $p_y$) orbitals of the bromide ions (Figure 8b). The $\sigma$-type overlap of $d_{xz}$ orbitals with the bromide ions can propagate the stronger antiferromagnetic interaction between induced spins on the copper ions than that in the $\pi$-type overlap for the tetrahedral coordination. Hence, the magnetic behavior of **4** can be interpreted as the sum of intradimer (intrachain) antiferromagnetic ($J_1 = -8.7$ cm$^{-1}$) and intrastack (intrachain) ferromagnetic ($J_2 = 1.5$ cm$^{-1}$) interactions.

## Conclusion

One of the purposes of this paper was to verify the validity of the halocuprate unit to increase dimensionality or nuclearity of the imino nitroxides. Imino nitroxide ligands in the complexes studied here have one-dimensional structures which are linked by the $Cu-X_2-Cu$ unit. The interchain magnetic couplings are mediated by the $Cu-X_2-Cu$ bond, and the strength of the antiferromagnetic interactions depends on the coordination geometry of the copper ions. In summary, the spin polarization is effective in **1**−**4**, while the SOMO−SOMO overlaps leading to the antiferromagnetic interaction are predominant in **2** and **3**. As a result, **1** and **4** show the intrachain ferromagnetic interaction, while **2** and **3** are the antiferromagnetic stacks.

**Acknowledgment.** This work was in part supported by a Grant-in-Aid for Scientific Research on Priority Area "Molecular Magnetism" (Area No. 228/No.06218203). Financial support by "Morino Foundation" is gratefully acknowledged.

**Supporting Information Available:** Tables SI−SXXI, listing X-ray data collection parameters, derived hydrogen positions, thermal parameters, and bond distances and angles, and ORTEP figures (31 pages). Ordering information is given on any current masthead page.

IC950663V

(31) Muller, E.; Piguet, C.; Bernardinelli, G.; Williams, A. F. *Inorg. Chem.* **1988**, *27*, 849.